

Enhanced antitumor efficacy of poly(D,L-lactide-co-glycolide)-based methotrexate-loaded implants on sarcoma 180 tumor-bearing mice

Li Gao^{1,2}
Lunyang Xia³
Ruhui Zhang¹
Dandan Duan³
Xiuxiu Liu²
Jianjian Xu²
Lan Luo¹

¹State Key Laboratory of Pharmaceutical Biotechnology, School of Life Sciences, Nanjing University, Nanjing, ²School of Biological and Medical Engineering, Hefei University of Technology, Hefei, ³Laboratory of Pharmaceutical Research, Anhui Zhongren Science and Technology Co., Ltd., Hefei, People's Republic of China

Correspondence: Lan Luo
State Key Laboratory of Pharmaceutical Biotechnology, School of Life Sciences, Nanjing University, 163 Xianlin Road, Nanjing, Jiangsu 210046, People's Republic of China
Tel +86 25 8368 6657
Fax +86 25 8368 6657
Email lanluo@nju.edu.cn

Jianjian Xu
School of Biological and Medical Engineering, Hefei University of Technology, 193 Tunxi Road, Hefei, Anhui 230009, People's Republic of China
Tel +86 551 6589 8316
Fax +86 551 6589 8316
Email xujianjian@hfut.edu.cn

Purpose: Methotrexate is widely used in chemotherapy for a variety of malignancies. However, severe toxicity, poor pharmacokinetics, and narrow safety margin of methotrexate limit its clinical application. The aim of this study was to develop sustained-release methotrexate-loaded implants and evaluate antitumor activity of the implants after intratumoral implantation.

Materials and methods: We prepared the implants containing methotrexate, poly(D,L-lactide-co-glycolide), and polyethylene glycol 4000 with the melt-molding technique. The implants were characterized with regards to drug content, morphology, in vitro, and in vivo release profiles. Differential scanning calorimetry (DSC) and Fourier transform infrared spectroscopy (FTIR) were carried out to investigate the physicochemical properties of the implants. Furthermore, the antitumor activity of the implants was tested in a sarcoma 180 mouse model.

Results: The implants were prepared as solid rods. Scanning electron microscopy images showed a smooth surface of the implant, suggesting that methotrexate was homogeneously dispersed in the polymeric matrix. The results of DSC and FTIR indicated that no significant interaction between methotrexate and the polymer was observed in the implants. Both in vitro and in vivo release profiles of the implants were characterized by burst release followed by sustained release of methotrexate. Intratumoral implantation of methotrexate-loaded implants could efficiently delay tumor growth. Moreover, an increase in the dose of implants led to a higher tumor suppression rate without additional systemic toxicity.

Conclusion: These results demonstrate that methotrexate-loaded implants had significant antitumor efficacy in a sarcoma 180 mouse model without dose-limiting side effects, and suggest that the implants could be potentially applied as an intratumoral delivery system to treat cancer.

Keywords: methotrexate, implant, sustained release, poly(D,L-lactide-co-glycolide), intratumoral chemotherapy

Introduction

Cancer is a major public health problem worldwide and it is the second leading cause of death in the United States. Around 1,688,780 new cancer cases and 600,920 cancer deaths are projected to occur in the United States in 2017.¹ In People's Republic of China, incidence and mortality of cancer have been increasing, and cancer has been the leading cause of death since 2010.² Systemic chemotherapy is the most commonly used method to treat cancers. However, it is often limited by the complex biology, cell type and doubling time, size, heterogeneity, location, and vascularization of tumors.³ Moreover, the toxicity has severely limited the safety and effectiveness of the conventionally systemic cancer chemotherapy.⁴

Local chemotherapy is considered as an effective way to increase the tumor specificity of chemotherapeutic drugs where anticancer drugs are released to the region containing the tumor or directly within the tumor.⁵ Local chemotherapy has been promoted by means of intratumoral chemotherapy, brachytherapy, debulking, photodynamic therapy, and aerosol chemotherapy.⁶ Polymer-based local drug delivery systems facilitate the delivery of antitumor drugs directly to the site of disease in a controlled manner and reduce the off-target tissue toxicities.⁷

Methotrexate (MTX) is a folate antagonist which interferes with the formation of DNA, RNA, and proteins. MTX is widely used to treat many solid tumors, including breast cancer, acute lymphatic leukemia, osteogenic sarcoma, choriocarcinoma, lung cancer, bladder carcinoma, brain medulloblastoma, primary central nervous system lymphoma, and chronic myeloid leukemia.^{8,9} MTX has also been used in the treatment of refractory rheumatoid arthritis and chronic inflammatory disorders.¹⁰ Conventional chemotherapy with MTX is administered periodically to maintain the therapeutic drug level in the body, which has serious side effects on the liver, lung, kidneys, gastrointestinal tract, and nervous system.¹¹ Furthermore, high doses of MTX, which are often used as cancer therapy, cause many severe toxic effects, such as myelosuppression, hepatic, renal, and pulmonary disorders. In some cases, the toxic effects are life-threatening.^{12,13}

The conventional MTX delivery systems include MTX injections and oral tablets. However, the severe toxicity, poor pharmacokinetics, and narrow safety margin of MTX limit the therapeutic outcome of the conventional drug delivery systems.⁸ Recently, many novel drug delivery systems have been developed to overcome the limitations of MTX with improved safety and efficacy of the drug. Examples include polymeric conjugates, microspheres, polymeric micelles, nanoparticles, dendrimers, hydrogels,⁸ implantable MTX films,¹⁴ and MTX poly(ϵ -caprolactone) implants.⁹

Poly(D,L-lactide-co-glycolide) (PLGA) has been approved by the US Food and Drug Administration (FDA) for the use of drug delivery, tissue engineering, medical, and surgical devices because of its biodegradability, biocompatibility, and sustained-release properties.¹⁵ In order to develop novel intratumoral delivery implants to overcome the limitations of MTX, we fabricated MTX-loaded implants using PLGA as the main polymer matrix with a melt molding method in the present study. The MTX-loaded implants were characterized in terms of morphology along with *in vitro* and *in vivo* drug release from the implants. To determine

the physicochemical properties of the drug, the implants were analyzed by differential scanning calorimetry (DSC) and Fourier transform infrared spectroscopy (FTIR). We further demonstrated that intratumoral delivery of MTX-loaded implants exhibited significant antitumor efficacy in a sarcoma 180 mouse model compared with intraperitoneal injection of MTX solution. It is interesting that increasing the dose of the implants led to higher tumor suppression rate (TSR) without additional systemic toxicity.

Material and methods

Chemicals and animals

MTX (purity 99.7%) was purchased from Huzhou Zhanwang Pharmaceutical Co., Ltd (Zhejiang, People's Republic of China). PLGA (75:25 lactide/glycolide; inherent viscosity 0.21 dL/g) was generously provided by Anhui Zhongren Science and Technology Co., Ltd. (Anhui, People's Republic of China). Other chemicals used: polyethylene glycol 4000 (PEG4000), from Beijing Huiyou Chemical Co., Ltd (Beijing, People's Republic of China); MTX injection, from Jiangsu Hengrui Medicine Co., Ltd. (Jiangsu, People's Republic of China); and high-performance liquid chromatography (HPLC)-grade acetonitrile, from Tedia Company, Inc. (Fairfield, OH, USA). Both RPMI-1640 medium and fetal calf serum were purchased from Hyclone (Logan, UT, USA). Ultra-pure water was obtained in a milli-Q system from EMD Millipore (Billerica, MA, USA). All chemicals, unless otherwise noted, were of analytical grade.

The mouse sarcoma 180 cells were obtained from the Cell Bank of Chinese Academy of Sciences (Shanghai, People's Republic of China). Healthy male Kunming mice (6–8 weeks) were purchased from Experimental Animal Center of Anhui Medical University (Hefei, People's Republic of China). The mice were kept at constant temperature ($23^{\circ}\text{C} \pm 2^{\circ}\text{C}$) and humidity ($50\% \pm 5\%$) and had free access to clean food and water. All animal protocols were approved by the Ethics Committee in Animal Experimentation at Nanjing University (Nanjing, People's Republic of China) and complied with the Guidelines for Care and Use of Laboratory Animals.

Preparation of MTX-loaded implants

The implants were prepared with a melt-molding technique under sterile conditions.⁹ Briefly, the dry powders containing 14.5% MTX, 75.5% PLGA, and 10% PEG4000 (w/w) were sieved and thoroughly blended. Then the homogenous mixture was heated at 80°C until it was completely melted.

The resultant blend was further molded into cylindrical implants. As a control, the blank implants were prepared in a similar manner without MTX.

Determination of drug content in the implants

Determination of drug content in the MTX-loaded implants was performed according to the method stated in the Pharmacopoeia of the People's Republic of China.¹⁶ Ten MTX-loaded implants were selected and weighed. Each implant sample was grounded in a pestle and mortar with a mixture of phosphate/citrate buffer (pH 6.0) and acetonitrile (90:10, v/v). The residue was further dissolved in an ultrasonic water bath for 20 min. The resulting suspension was centrifuged at 12,000 rpm for 10 min.¹⁷ Subsequently, an aliquot of the supernatant (20 μ L) was analyzed by HPLC. The actual drug content of each implant was then calculated.

Characterization of MTX-loaded implants

Scanning electron microscopy (SEM)

The surface and cross-section of the implants were examined using a JEOL JSM-6490LV scanning electron microscope (JEOL, Tokyo, Japan) operating at a voltage of 20 kV. The implant was cut with a sharp scalpel to observe morphology of the cross-section. Prior to imaging, all samples were placed on metal sample holders and coated with gold for 90 s at 20 mA using JEOL JFC-1600 auto fine coater (JEOL). The external and internal morphologies were imaged at $\times 1,000$ magnification. The photomicrographs were adjusted using Adobe Photoshop 6.0 (Adobe Systems Incorporated, San Jose, CA, USA) and CorelDRAW 12 (Corel Corporation, Ottawa, Canada).

DSC analysis

DSC analysis was carried out with a thermal analysis instrument (Q2000; TA Instruments, New Castle, DE, USA). Samples (5 mg) of MTX-loaded implants, pure PLGA, PEG4000, MTX, and physical mixture of PLGA, PEG4000, and MTX were sealed in aluminum pans and measured by DSC at a heating rate of $10^{\circ}\text{C min}^{-1}$ over a temperature range of 25°C – 300°C . High purity nitrogen was used as the purge gas at a flow rate of 50 mL/min.

FTIR

Infrared spectra were generated in an FTIR spectrophotometer (Nicolet 6700; Thermo Fisher Scientific, Waltham, MA, USA). Measurements were carried out using the attenuated

total reflectance technique. Each spectrum was a result of 32 scans with a resolution of 4 cm^{-1} .

In vitro release assay

The in vitro release assay was performed using the rotating basket method on a dissolution apparatus. Fifty milligram implants were placed in 250 mL of release medium with PBS (pH 7.4). The rotating speed of the basket was set at 100 rpm and the temperature of the release medium was maintained at $37^{\circ}\text{C} \pm 0.5^{\circ}\text{C}$. At different time points (1, 2, 3, 4, 5, 6, 7, 8, 9, 10, and 11 days), 5 mL of the sample was withdrawn, centrifuged at 12,000 rpm for 10 min, and stored at 4°C until analysis. Then 5 mL of fresh release medium was immediately added back to the dissolution flask to maintain a constant sink condition. HPLC was used for the quantitative determination of MTX. The measurement was performed in triplicate for each batch.

In vivo release assay

To determine the release rate of MTX implants in vivo, 5 to 6-week-old female Wistar rats were implanted intramuscularly with two MTX-loaded implants containing approximately 0.25 mg MTX into the right leg. At predetermined time intervals (1, 3, 5, 7, 10, 15, and 20 days), the rats were euthanized by CO_2 asphyxiation and the implants were retrieved, rinsed with deionized water, dried under vacuum, and stored at 4°C until analysis. Three animals were used at each time point. The amount of drug in the residual implant was determined by HPLC. The in vivo cumulative release percentage of MTX was calculated as follows:

$$\text{MTX release percentage (\%)} = \frac{\text{Initial MTX amount} - \text{Residual MTX amount}}{\text{Initial MTX amount}} \times 100$$

In vitro degradation study

The in vitro degradation was measured by recording the weight loss of the blank implants (without MTX) in PBS (pH 7.4). The implants were placed in different tubes containing 3 mL of PBS. Those tubes were placed in an incubator shaker agitated at 30 rpm with a temperature of 37°C . At the predetermined time points (7, 14, 21, 28, 35, 42, 49, 56, 63, 70, and 77 days), the implants were retrieved from the PBS, rinsed with deionized water, and vacuum-dried for 48 h. The percentage of weight loss was obtained by the ratio between the weight loss and the initial weight of the dry sample at each time point ($n=6$).

The HPLC method for determination of MTX in the implants

The HPLC system (Shimadzu, Kyoto, Japan) was equipped with two LC-15C pumps, an SPD-15C essential UV detector, and a CTO-15C essential column oven. A Hypersil BDS C6H5 column (250×4.6 mm, 5 µm particle size) was used as an analytical column and maintained at 25°C in the column oven. The mixture of phosphate/citrate buffer (pH 6.0) and acetonitrile (90:10, v/v) was used as the mobile phase and the flow rate was 1.0 mL/min.¹¹ The injection volume was 20 µL and the absorbance was detected at 302 nm. The external standard method was used for quantitative analysis.¹⁶

Antitumor efficacy of MTX-loaded implants

Cell culture and sarcoma 180 mouse tumor model

The mouse sarcoma 180 cells were cultured in RPMI-1640 medium supplemented with 10% fetal calf serum, penicillin (100 U/mL), and streptomycin (100 µg/mL). Cells were incubated in a humidified incubator with 5% CO₂ and 95% air at 37°C. The cell suspension was adjusted to 1×10⁷ cells/mL, from which 100 µL of cell culture medium was injected subcutaneously into the armpit of right anterior limb of each mouse. The study was started when the tumor volume reached 50–60 mm³.

Antitumor activity in vivo

Thirty tumor-bearing Kunming mice weighing approximately 25 g were randomly divided into five groups (n=6 per group): i) single intratumoral implantation of blank implants as negative control group, ii) intraperitoneal injection of MTX solution at the dose of 4 mg/kg as positive control group, iii) single intratumoral implantation of MTX-loaded implants at the dose of 1 mg/kg (MTX implant-L group), iv) single intratumoral implantation of MTX-loaded implants at the dose of 2 mg/kg (MTX implant-M group), and v) single intratumoral implantation of MTX-loaded implants at the dose of 4 mg/kg (MTX implant-H group). The doses were given according to the exploration test on tolerance of MTX in tumor-bearing mice. The hair near the solid tumor was shaved and the skin was disinfected with 70% ethanol. The implants were then inserted into the center of the tumor using the modified 17 gauge trochar provided by Anhui Zhongren Science and Technology Co. The tumor volumes were measured every other day using digital caliper and calculated by the formula

$$V \text{ (mm}^3\text{)} = \text{Length} \times (\text{width}^2)/2.^{18}$$

At the end of the study, the mice were sacrificed and the tumors were collected and weighed. In addition, the TSR was calculated using the formula

$$\text{TSR} = (1 - \text{Wt/Wc}) \times 100\%,$$

where Wt and Wc represent the mean final tumor weight of treated group and negative control group, respectively.¹⁹ The condition with a tumor size exceeding 20 mm in any direction was considered as a humane endpoint.²⁰

Histopathological studies

At predetermined time points (on day 7 and 14 after treatment), one mouse in each group was sacrificed and the liver and kidney tissues were isolated. The tissues were fixed in neutral 10% formalin solution and then dehydrated in a graded ethanol series. The tissues were embedded in paraffin and sectioned at 5 µm thickness. Tissue slides were stained with hematoxylin and eosin for histopathological examination. The histology images were taken using an Olympus BX51 microscope system (Olympus Corporation, Tokyo, Japan). The histopathological examination of all tissues was carried out in a blinded fashion by a pathologist who was unaware of the treatment groups.

Statistical analysis

Statistical analyses were performed using a one-way ANOVA where a *P*-value of less than 0.05 was considered statistically significant. All the data were expressed as mean ± SD and analyzed using GraphPad Prism version 5.0 (GraphPad Software, Inc., La Jolla, CA, USA). One-way ANOVA with Tukey's multiple comparison test was used to compare the means of all the experimental groups.

Results

Preparation of MTX-loaded implants

The MTX-loaded implants were prepared by blending and melting the mixture of MTX, PLGA, and PEG4000. The implants were further molded into solid cylinders with the average diameter of 0.88±0.01 mm and length of 2.27±0.13 mm (Figure 1). Moreover, the average weight of the implants was 1.68±0.12 mg (n=10). The mean actual drug content of the tested implants was (15.05%±0.15%), which was close to the number in the label claim of the drug (14.5%, w/w).

Morphology of MTX-loaded implants

SEM was used to evaluate the microstructure of the MTX-loaded implants. Both the external surface (Figure 2A) and



Figure 1 Macroscopic picture of MTX-loaded implants.
Abbreviation: MTX, methotrexate.

the internal surface (Figure 2B) of the blank implant (without drug) were smooth. The external surface of the implant was found to be smooth and homogenous (Figure 2C). Furthermore, the implant was cut with a scalpel to observe morphology of the cross-section. The cross-section of the

implant was a little rough under SEM but still homogenous without obvious pores or channels (Figure 2D).

DSC analysis

Thermal behaviors of MTX, PLGA, PEG4000; physical mixture of MTX, PLGA, and PEG4000; and MTX-loaded implants were analyzed by DSC (Figure 3). The curve of pure MTX (Figure 3A) showed an endotherm in the temperature between 120°C and 150°C which can probably be attributed to the desolvation of the drug. Furthermore, a broad exothermic peak in the range 240°C to 260°C was observed, which was probably due to the decomposition of the MTX. The DSC traces of PLGA (Figure 3B) and PEG4000 (Figure 3C) exhibited a melting sharp endothermic peak centered at approximately 69°C and 60°C, respectively. The DSC curves for physical mixture of MTX, PLGA, and PEG4000 (Figure 3D) and MTX-loaded implants (Figure 3E) showed a thermal behavior similar to that identified for pure MTX and the polymers.

FTIR studies

FTIR spectra analysis of MTX, PLGA, PEG4000, physical mixture of MTX, PLGA, and PEG4000, and MTX-loaded implants revealed characteristic absorption bands at different frequencies (Figure 4). As shown in the FTIR spectrum

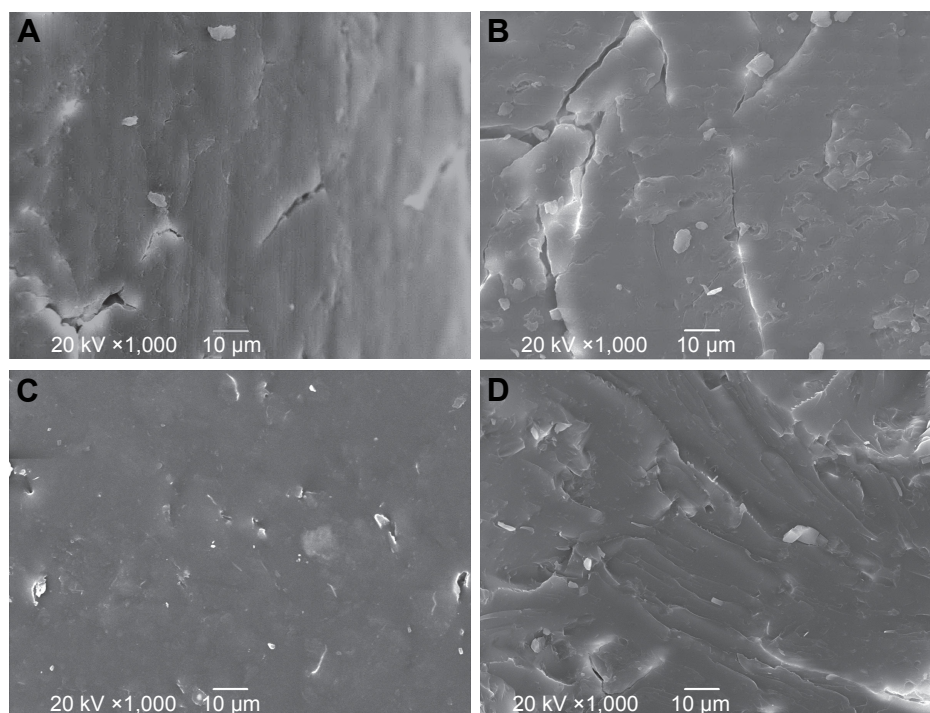


Figure 2 SEM images of the (A) external surface and (B) cross-section of the blank implant, and (C) external surface and (D) cross-section of the MTX-loaded implants (magnification $\times 1,000$).

Abbreviations: MTX, methotrexate; SEM, scanning electron microscopy.

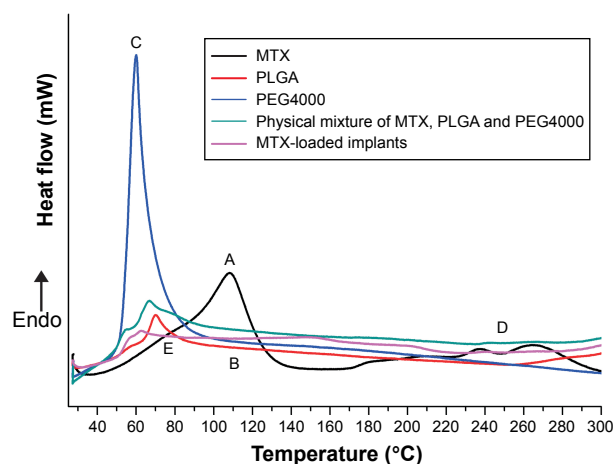


Figure 3 DSC curves of (A) MTX, (B) PLGA, (C) PEG4000, (D) physical mixture of MTX, PLGA, and PEG4000, and (E) MTX-loaded implants.

Abbreviations: DSC, differential scanning calorimetry; Endo, endothermic; MTX, methotrexate; PEG, polyethylene glycol; PLGA, poly(D,L-lactide-co-glycolide).

of MTX (Figure 4A), a broad band at $3,367\text{ cm}^{-1}$ was attributed to the stretching vibration of N–H.^{9,21,22} Typical infrared absorption bands observed in PLGA (Figure 4B) and PEG4000 (Figure 4C) were detected in the spectra of physical mixture of MTX, PLGA, and PEG4000 (Figure 4D) and MTX-loaded implants (Figure 4E).

In vitro and in vivo drug release from the implants

The in vitro cumulative release test was carried out in the release medium under a suitable sink condition (Figure 5A). We found that approximately 20% of drug was released on

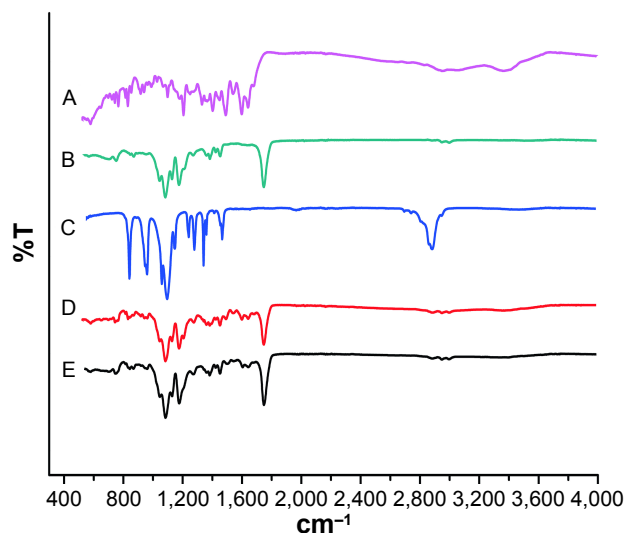


Figure 4 FTIR spectra of (A) MTX, (B) PLGA, (C) PEG4000, (D) physical mixture of MTX, PLGA, and PEG4000, and (E) MTX-loaded implants.

Abbreviations: FTIR, Fourier transform infrared spectroscopy; MTX, methotrexate; PEG, polyethylene glycol; PLGA, poly(D,L-lactide-co-glycolide).

the first day. Subsequently, the drug was released from the implants almost at a constant rate. The mean cumulative release percentage reached 60% on day 4. From day 5, the drug release rate gradually slowed down. As a whole, the cumulative release reached an average of 86% within 11 days. To gain the information of the in vivo release profile (Figure 5B), the MTX-loaded implants were implanted intramuscularly into the right leg of the rats and then the implants were collected on days 1, 3, 5, 7, 10, 15, and 20 post-implantation. The MTX-loaded implants released approximately 17% of the drug on the first day and 42.3% of the drug within 5 days. The mean cumulative release percentage reached 74% on day 10. Finally, almost 95% of the MTX was released from the implants in 20 days.

In vitro degradation

The in vitro degradation of the blank implants (without MTX) in phosphate buffer solution at 37°C was analyzed over 11 weeks. As shown in the degradation curve (Figure 6), the samples lost mass from the first week of degradation. Furthermore, the samples lost almost 80% of their original weight at 11 weeks.

Antitumor efficacy

The evaluation of antitumor activity was conducted in Kunming mice inoculated with sarcoma 180 cell lines. As shown in the tumor growth curve (Figure 7A), the tumor had grown rapidly in the blank implant group and the tumor size exceeded 3.6 cm^3 on day 20 post-implantation. The MTX-loaded implants delayed tumor growth effectively. When the high-dose MTX-loaded implants were used, we observed more significant tumor growth inhibition compared with other groups. Throughout the course of the experiment, the body weights of all mice increased slowly but there was no significant difference among the groups (Figure 7B).

At the end of the experiment (day 20 post-implantation), mice were sacrificed and tumors dissected from the mice were weighed (Figure 7C). The mean final tumor weight of the blank implant group was $4.5 \pm 1.8\text{ g}$ and $3.1 \pm 1.4\text{ g}$ in MTX solution group. The mean final tumor weights were $1.9 \pm 1.0\text{ g}$ and $1.8 \pm 0.9\text{ g}$ for MTX implant-L and MTX implant-M groups, respectively. Furthermore, the mice in MTX implant-H group had an average tumor weight of $1.0 \pm 0.6\text{ g}$ (Table 1). The tumor weight of MTX implant-H group was significantly lower than other groups. The TSR of MTX implant-L group (58%) was greater than that in MTX solution group (31%). The TSR of MTX implant-H group rose to 78% which was significantly higher than any other

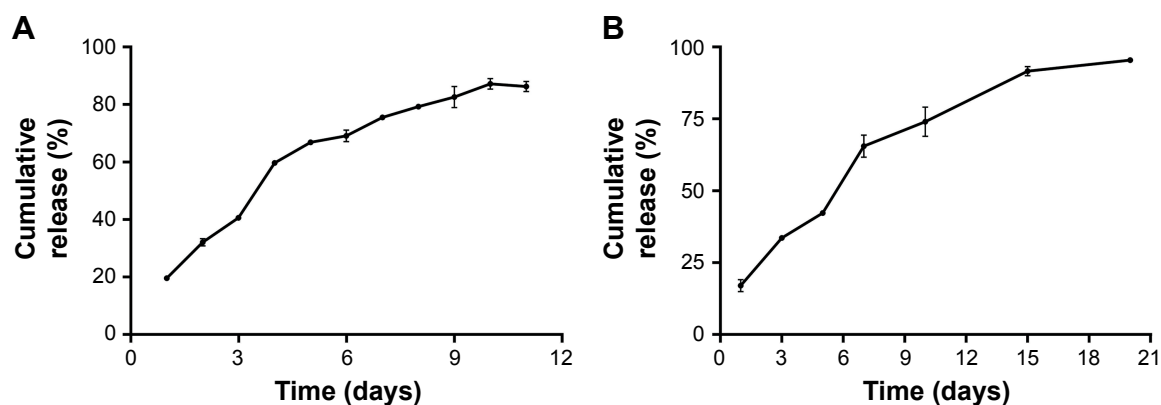


Figure 5 The (A) in vitro and (B) in vivo cumulative release profiles of MTX from the implants.

Note: Data are shown as mean \pm SD (n=3).

Abbreviation: MTX, methotrexate.

group ($P < 0.05$). Additionally, all the mice survived until the end of the experiment.

To further evaluate the systemic toxicity of MTX-loaded implants on the mice, histopathological studies of the liver and kidney from the sarcoma 180 tumor-bearing mice were carried out on day 14 after treatment. As shown in the typical histopathological images (Figure 8), mild inflammatory cell infiltration and spotty necrosis were observed both in the MTX solution treated group and the MTX implant-H treated group. Furthermore, we did not find obvious necrosis in the major organs from both MTX solution treated group and MTX implant-H treated group.

Discussion

MTX has been widely used in the treatment of many neoplastic disorders. Systemic administration of MTX induces several dose-related side effects which often force the patients to lower the MTX dose or switch to a different drug.²³ There is an urgent need to find a new drug delivery system to overcome

the limitations facing MTX. MTX is a cell-cycle phase specific drug, and prolonged exposure of the drug to the cancer cells is necessary to yield superior antitumor efficacy.¹⁴ In this study, we developed sustained-release MTX-loaded implants which focused therapy directly on the tumor site to enhance the antitumor efficacy and minimize the treatment-related side effects.

PLGA was the main excipient used in the fabrication of the MTX-loaded implants. PLGA is a copolymer of polylactic acid and polyglycolic acid which have been widely used in drug delivery systems, tissue engineering, and medical and surgical devices. PLGA is approved by the FDA in the US for therapeutic applications because of its biodegradability, biocompatibility, and sustained-release properties.^{15,24} PEG4000 was the other excipient of the implants which was characterized by low melting point, low toxicity, wide drug compatibility and hydrophilicity. PEG has been widely used as a drug carrier and addition of PEG can facilitate the dissolution and increase the release rate of the drug from implants by promoting the water diffusion into the implants.^{25–27}

The morphology of the implant has a significant impact on the drug release rate of drug delivery systems.²⁸ The SEM images showed that the external and internal surfaces of the MTX-loaded implants were homogenous. These results suggested that the fabrication procedure of the implants yielded a uniform distribution of the drug into the polymeric matrix.⁹

DSC is the most common thermal analysis technique used to examine the physical properties of implants. Consistent with previous findings,^{9,29} our DSC thermogram of MTX-loaded implants showed all endothermic events corresponding to MTX, PLGA, and PEG4000. The FTIR analysis of MTX was performed to observe the characteristic vibrations of COOH, NH₂, CH₂, and phenyl ring.²¹ Typical infrared absorption bands of the functional groups visualized in pure MTX were observed

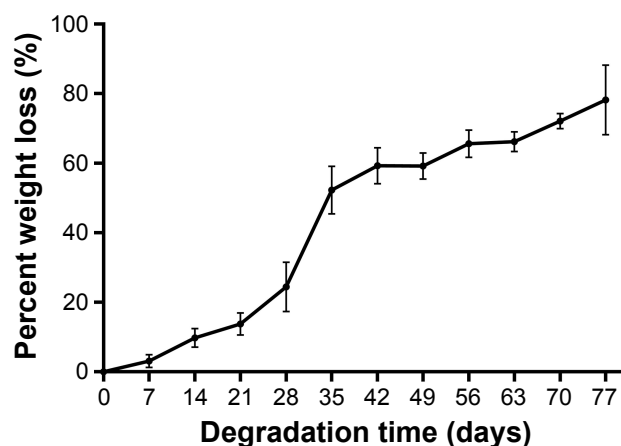


Figure 6 In vitro weight loss of the blank implants (without drug).

Note: Data are shown as mean \pm SD (n=6).

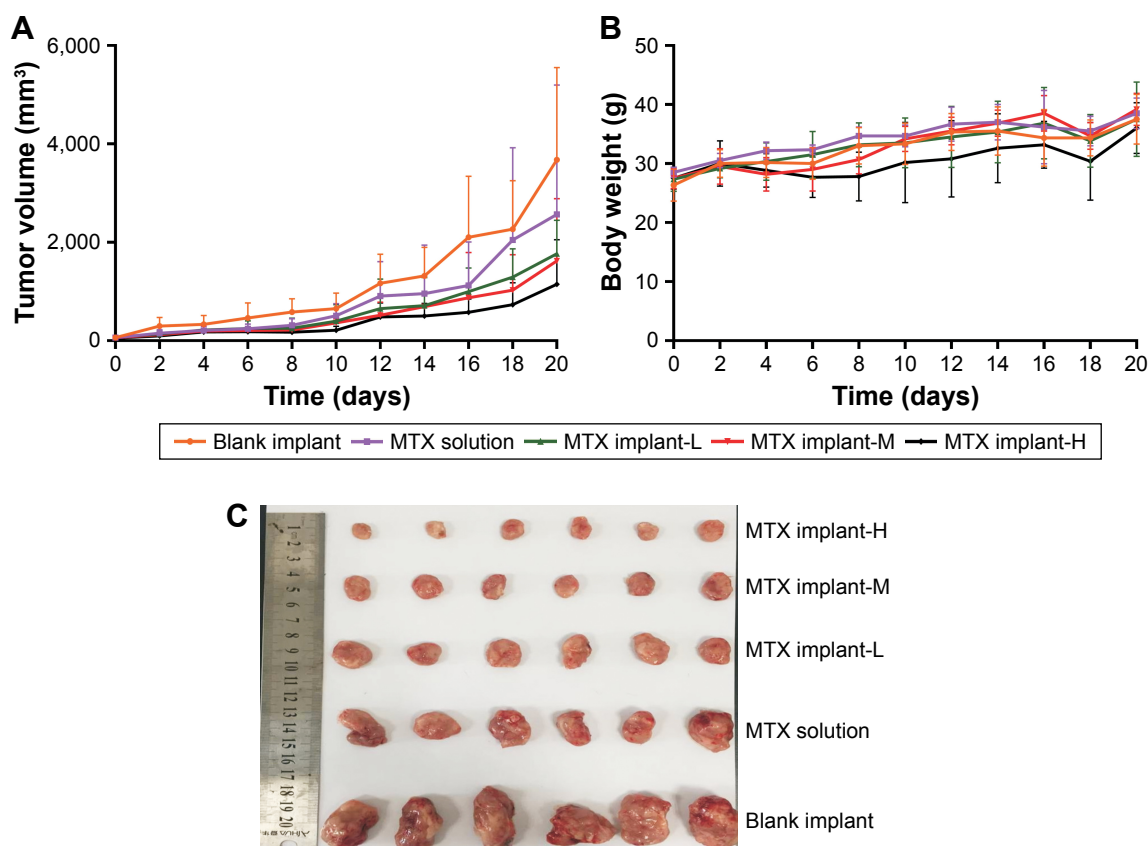


Figure 7 Antitumor efficacy of MTX-loaded implants on sarcoma 180 tumor-bearing mice.

Notes: (A) Tumor growth curve of the tumor-bearing mice. (B) The average body weight of the mice during the treatment period. (C) Picture of tumors dissected from the mice on day 20 post-implantation. MTX implant-H is MTX-loaded implants at the dose of 4 mg/kg; MTX implant-M is MTX-loaded implants at the dose of 2 mg/kg; and MTX implant-L is MTX-loaded implants at the dose of 1 mg/kg.

Abbreviation: MTX, methotrexate.

in the FTIR spectra of the MTX-loaded implants and physical mixture of MTX, PLGA, and PEG4000. The FTIR results were also consistent with those previously described.^{9,22} Moreover, we did not observe new bands in the FTIR spectra of MTX-loaded implants. Therefore, the FTIR data are in agreement with the DSC analysis results, supporting that no chemical interactions occurred between the drug and the polymers during the manufacturing process of the implants.

The drug release from the implants depends on the environmental conditions, physicochemical properties of

the drug and polymers, the shape, size, and drug loading of implants.^{28,30} The drug release from MTX-loaded implants exhibited an initial burst followed by sustained-release both in vitro and in vivo. The initial burst release may be due to fast dissolution and diffusion of MTX accumulated on the surface of the implants. The following sustained release of the drug could be explained by the fact that MTX was gradually diffused in the matrix and released from the implants. The duration of the in vivo drug release became longer compared with the in vitro release. This phenomenon could be due to the difference between the in vivo physiological environment and the in vitro simulated physiological environment.⁹ It is generally expected that the optimal drug release profile for intratumoral implants should have an initial burst release of a large amount of the drug so that it can rise to the therapeutic concentration rapidly, followed by sustained release to maintain the therapeutic concentration for a prolonged period.⁵ The therapeutic effect of MTX is primarily attributed to inhibition of human DHFR.³¹ Thus, prolonged exposure of MTX to cancerous cells will produce

Table 1 The TSR of each group

Groups	Mean tumor weight (g)	TSR (%)
Blank implant	4.5±1.8	
MTX solution	3.1±1.4	31
MTX implant-L	1.9±1.0	58
MTX implant-M	1.8±0.9	60
MTX implant-H	1.0±0.6	78

Notes: MTX implant-L is MTX-loaded implants at the dose of 1 mg/kg; MTX implant-M is MTX-loaded implants at the dose of 2 mg/kg; and MTX implant-H is MTX-loaded implants at the dose of 4 mg/kg.

Abbreviations: MTX, methotrexate; TSR, tumor suppression rate.

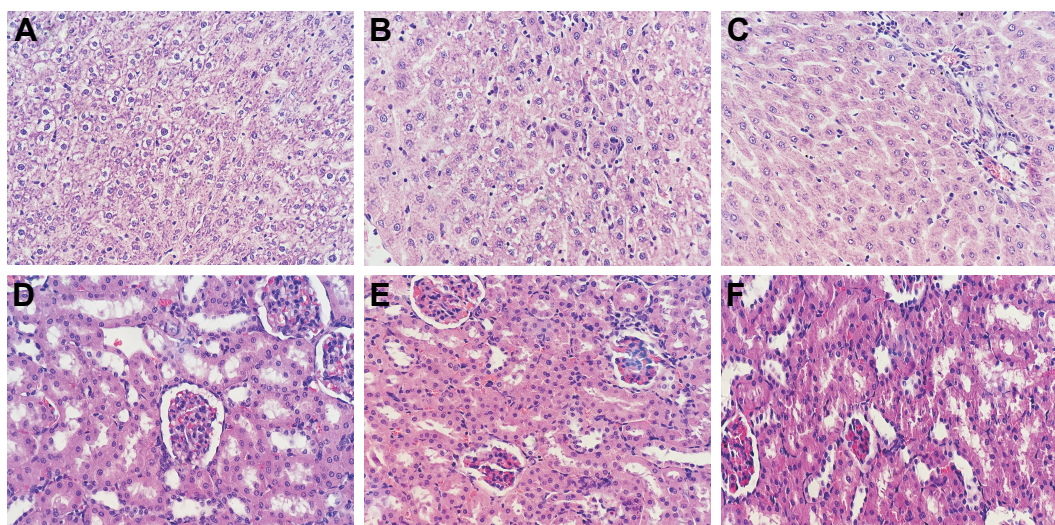


Figure 8 Typical histopathological images of major organs of sarcoma 180 tumor-bearing mice (magnification $\times 400$).

Notes: (A) Normal morphology of liver, (B) liver tissue of mouse receiving intraperitoneal injection of MTX solution, (C) liver tissue of mouse receiving intratumoral implantation of high doses of MTX-loaded implants, (D) normal morphology of kidney, (E) kidney tissue of mouse receiving intraperitoneal injection of MTX solution, (F) kidney tissue of mouse receiving intratumoral implantation of high doses of MTX-loaded implants.

Abbreviation: MTX, methotrexate.

a longer period of DHFR inhibition and increase anticancer efficacy of MTX.³²

In this study, we investigated the antitumor efficacy of MTX-based implants using a sarcoma 180 mouse tumor model. We found that the MTX-loaded implants delayed tumor growth efficiently. The total dose administered via the high-dose MTX-loaded implants was equivalent to the total amount administered intraperitoneally. A more significant decrease in tumor size in the MTX-loaded implant treated groups indicated that animals receiving MTX-loaded implants exhibited much superior tumor growth inhibition than those receiving an equivalent dose of free MTX systemically. In addition, we did not observe any significant difference in body weight among the groups. Moreover, the histopathological analyses revealed no significant damage to the major organs of mice treated with high doses of MTX-loaded implants, indicating that the MTX-loaded implants did not have additional side effects on the animals. Further, we found that TSR increased when higher doses of MTX-loaded implants were used. Very likely, a larger amount of MTX was released from the implants, and accumulated in the tumor site, which resulted in strong antitumor efficacy. The tumor growth curve indicated that MTX-loaded implants could inhibit tumor growth in a dose-dependent manner *in vivo*.

Conclusion

In the present study, we prepared PLGA-based MTX-loaded implants with a melt-molding technique. The implants were prepared as cylinders and the mean drug content of the

implants was $(15.05\% \pm 0.15\%)$. The SEM results indicated that MTX was homogeneously dispersed in the polymeric matrix. The DSC and FTIR data supported the notion that no detectable chemical interactions occurred between the drug and the polymers. Release of MTX from the implants, both *in vitro* and *in vivo*, was characterized by initial high burst release followed by sustained-release of the drug. Results from intratumoral implantation of MTX-loaded implants into the Kunming mice bearing sarcoma 180 demonstrated that the implants had a significant antitumor activity on the sarcoma 180 mouse model. Furthermore, an increase in the dose of the implants led to a higher TSR without additional systemic toxicity. We conclude that the PLGA-based MTX-loaded implants have the potential to be used as a new intratumoral drug delivery system to treat cancer with high antitumor efficiency and low systemic toxicity.

Acknowledgments

This work was funded by the National Science and Technology Support Program of China under Grant no 2013BAI01B00. The authors thank Prof Lili Xu for writing assistance and Dr Yang Zhao for histopathological analysis. The authors also acknowledge Prof Shiliang Wang for his assistance in the experiment of fabrication of the MTX-loaded implants.

Author contributions

LG, JJX, and LL designed the experiment. LG, LYX, RHZ, DDD, and XXL conducted the experiments and data analysis,

LG drafted the manuscript. All authors contributed toward data analysis, drafting and revising the paper and agree to be accountable for all aspects of the work.

Disclosure

The authors report no conflicts of interest in this work. The authors alone are responsible for the content and writing of this article.

References

1. Siegel RL, Miller KD, Jemal A. Cancer Statistics, 2017. *CA Cancer J Clin.* 2017;67(1):7–30.
2. Chen W, Zheng R, Baade PD, et al. Cancer statistics in China, 2015. *CA Cancer J Clin.* 2016;66(2):115–132.
3. Saltzman WM, Fung LK. Polymeric implants for cancer chemotherapy. *Adv Drug Deliv Rev.* 1997;26(2–3):209–230.
4. Goldberg EP, Hadba AR, Almond BA, Marotta JS. Intratumoral cancer chemotherapy and immunotherapy: opportunities for nonsystemic pre-operative drug delivery. *J Pharm Pharmacol.* 2002;54(2):159–180.
5. Weinberg BD, Blanco E, Gao J. Polymer implants for intratumoral drug delivery and cancer therapy. *J Pharm Sci.* 2008;97(5):1681–1702.
6. Hohenforst-Schmidt W, Zarogoulidis P, Darwiche K, et al. Intratumoral chemotherapy for lung cancer: re-challenge current targeted therapies. *Drug Des Devel Ther.* 2013;7:571–583.
7. Wolinsky JB, Colson YL, Grinstaff MW. Local drug delivery strategies for cancer treatment: gels, nanoparticles, polymeric films, rods, and wafers. *J Control Release.* 2012;159(1):14–26.
8. Abolmaali SS, Tamaddon AM, Dinarvand R. A review of therapeutic challenges and achievements of methotrexate delivery systems for treatment of cancer and rheumatoid arthritis. *Cancer Chemother Pharmacol.* 2013;71(5):1115–1130.
9. Pereira Ade F, Pereira LG, Barbosa LA, et al. Efficacy of methotrexate-loaded poly(epsilon-caprolactone) implants in Ehrlich solid tumor-bearing mice. *Drug Deliv.* 2013;20(3–4):168–179.
10. Genestier L, Paillot R, Quemeneur L, Izeradjene K, Revillard JP. Mechanisms of action of methotrexate. *Immunopharmacology.* 2000;47(2–3):247–257.
11. Misra R, Mohanty S. Sustained release of methotrexate through liquid-crystalline folate nanoparticles. *J Mater Sci Mater Med.* 2014;25(9):2095–2109.
12. Gaies E, Jebabli N. Methotrexate Side Effects: Review Article. *J Drug Metab Toxicol.* 2012;3(4):1–5.
13. Al-Quteimat OM, Al-Badaineh MA. Practical issues with high dose methotrexate therapy. *Saudi Pharm J.* 2014;22(4):385–387.
14. Singh UV, Pandey S, Umadevi P, Udupa N. Preparation, characterization, and antitumor efficacy of biodegradable poly(lactic acid) methotrexate implantable films. *Drug Delivery.* 1997;4(2):101–106.
15. Kapoor DN, Bhatia A, Kaur R, Sharma R, Kaur G, Dhawan S. PLGA: a unique polymer for drug delivery. *Ther Deliv.* 2015;6(1):41–58.
16. The State Pharmacopoeia Commission of People's Republic of China. *The Pharmacopoeia of the People's Republic of China.* Beijing: China Medical Science Press; 2015.
17. Gao L, Xie C, Du Y, et al. Characterization and antitumor efficacy of poly(L-lactid acid)-based etoposide-loaded implants. *Drug Deliv.* 2017;24(1):765–774.
18. Dong Y, Chin SF, Blanco E, et al. Intratumoral delivery of beta-lapachone via polymer implants for prostate cancer therapy. *Clin Cancer Res.* 2009;15(1):131–139.
19. Dong W, Zhang L, Niu Y, et al. A stable and practical etoposide-containing intravenous long-/medium-chain triglycerides-based lipid emulsion formulation: pharmacokinetics, biodistribution, toxicity, and antitumor efficacy. *Expert Opin Drug Deliv.* 2013;10(5):559–571.
20. Mitchell DA, Cui X, Schmittling RJ, et al. Monoclonal antibody blockade of IL-2 receptor alpha during lymphopenia selectively depletes regulatory T cells in mice and humans. *Blood.* 2011;118(11):3003–3012.
21. Ayyappan S, Sundaraganesan N, Aroulmoji V, Murano E, Sebastian S. Molecular structure, vibrational spectra and DFT molecular orbital calculations (TD-DFT and NMR) of the antiproliferative drug Methotrexate. *Spectrochim Acta A Mol Biomol Spectrosc.* 2010;77(1):264–275.
22. Gharebaghi F, Dalali N, Ahmadi E, Danafar H. Preparation of wormlike polymeric nanoparticles coated with silica for delivery of methotrexate and evaluation of anticancer activity against MCF7 cells. *J Biomater Appl.* 2017;31(9):1305–1316.
23. de Fatima Pereira A, Mara da Costa V, Cristina Magalhaes Santos M, et al. Evaluation of the effects of methotrexate released from polymeric implants in solid Ehrlich tumor. *Biomed Pharmacother.* 2014;68(3):365–368.
24. Xu Y, Kim CS, Saylor DM, Koo D. Polymer degradation and drug delivery in PLGA-based drug-polymer applications: a review of experiments and theories. *J Biomed Mater Res B Appl Biomater.* 2017;105(6):1692–1716.
25. El-Badry M, Fetih G, Fathy M. Improvement of solubility and dissolution rate of indomethacin by solid dispersions in Gelucire 50/13 and PEG4000. *Saudi Pharm J.* 2009;17(3):217–225.
26. Cheng L, Lei L, Guo S. In vitro and in vivo evaluation of praziquantel loaded implants based on PEG/PCL blends. *Int J Pharm.* 2010;387(1–2):129–138.
27. Wang K, Zhang X, Zhang L, et al. Development of biodegradable polymeric implants of RGD-modified PEG-PAMAM-DOX conjugates for long-term intratumoral release. *Drug Deliv.* 2015;22(3):389–399.
28. Solano AG, de Fatima Pereira A, Pinto FC, et al. Development and evaluation of sustained-release etoposide-loaded poly(epsilon-caprolactone) implants. *AAPS PharmSciTech.* 2013;14(2):890–900.
29. Chadha R, Arora P, Kaur R, Saini A, Singla ML, Jain DS. Characterization of solvatomorphs of methotrexate using thermoanalytical and other techniques. *Acta Pharm.* 2009;59(3):245–257.
30. Li C, Cheng L, Zhang Y, Guo S, Wu W. Effects of implant diameter, drug loading and end-capping on praziquantel release from PCL implants. *Int J Pharm.* 2010;386(1–2):23–29.
31. Wong PT, Choi SK. Mechanisms and implications of dual-acting methotrexate in folate-targeted nanotherapeutic delivery. *Int J Mol Sci.* 2015;16(1):1772–1790.
32. Rotman M, Rosenthal CJ. *Concomitant Continuous Infusion Chemotherapy and Radiation.* 1st ed. Berlin Heidelberg: Springer-verlag; 1991.

→ Video abstract



Point your SmartPhone at the code above. If you have a QR code reader the video abstract will appear. Or use:

<http://youtu.be/b4QqgEj0A4o>

Drug Design, Development and Therapy

Dovepress

Publish your work in this journal

Drug Design, Development and Therapy is an international, peer-reviewed open-access journal that spans the spectrum of drug design and development through to clinical applications. Clinical outcomes, patient safety, and programs for the development and effective, safe, and sustained use of medicines are the features of the journal, which

has also been accepted for indexing on PubMed Central. The manuscript management system is completely online and includes a very quick and fair peer-review system, which is all easy to use. Visit <http://www.dovepress.com/testimonials.php> to read real quotes from published authors.

Submit your manuscript here: <http://www.dovepress.com/drug-design-development-and-therapy-journal>